ELSEVIER

Journal of Organometallic Chemistry 535 (1997) 135–141

Journal of Organometallic Chemistry

1,1′-Substituted pyridinothiaferrocene derivatives

Niki Sachsinger *, C. Dennis Hall

Department of Chemistry, King's College, Strand, London WC2R 2LS, UK

Received 25 October 1996; revised 29 November 1996

Abstract

The syntheses and characterisation of three new ferrocene ligands containing N and S as heteroatoms are described. In addition, the coordination of guest metal cations into each host binding site has been studied by spectroscopic and electrochemical methods and the results for zinc complexation are presented. © 1997 Elsevier Science S.A.

1. Introduction

The chemistry of azathiaferrocene ligands and their transition metal complexes has been of general interest for more than 30 years [1]. Nonetheless, very few examples of pyridinothiaferrocenes are known [2]. We are currently interested in the coordination properties of ferrocene ligands incorporating sulphur and pyridine or bipyridyl units [3] since complexes with suitable cations (e.g. Zn^{2+}) may afford catalysts for a variety of hydrolytic reactions. This paper reports the synthesis and characterisation of three novel 1,1′-bis(pyridine) derivatives of ferrocene and their complexation with zinc and copper.

2. Experimental

^{1}H and ^{13}C NMR spectra were recorded on either Bruker AM360 or Bruker WX400 spectrometers. Mass spectra were obtained using FAB with a thioglycerol or 3-NBA matrix on a Kratos MS890MS instrument at the ULIRS Mass Spectrometry Service, King's College, London. Exact mass was determined by the chemical ionisation technique. UV spectra were recorded on a Hewlett-Packard diode array spectrometer (Model no. 8452A) using 1 mm and 10 mm path length quartz cuvettes. Cyclic voltammograms were recorded at 293 K using an EG&G Model 273 potentiostat with Model 270 software controlled by a Viglen computer connected to a Hewlett-Packard colour plotter for graphical output. The cyclic voltammetry experiments were conducted in dry, nitrogen-purged CH_3CN with 0.1 M Bu_4NClO_4 as supporting electrolyte, Ag/AgCl (sat. AgCl in 3 M NaCl) as the reference electrode and Pt wire as both counter and working electrode. The scan rate was normally $100\,mV\,s^{-1}$ with *IR* compensation applied during each scan.

2.1. Preparative details

1,10-Dithia[2](2,6)pyridino-ferrocenophane **4** was obtained as reported by Sato et al. [4] to give an orange solid with m.p. 155–160 °C (m.p. 162–163 °C [4]). 1,1′-Bis(hydroxymethyl)ferrocene was synthesised by reduction of 1,1′-ferrocenedialdehyde [5] with lithium aluminiumhydride; 1,1′-ferrocenedithiol [6] and 2-bromomethylpyridine [7] were prepared according to literature procedures. 2-Mercaptomethylpyridine [8] was prepared from 2-chloromethylpyridine [9].

2-Mercaptopyridine and 2-pyridinemethanol were purchased from Aldrich and used as supplied.

2.2. Synthesis of 1,1′-bis(2-pyridylmercaptomethyl)ferrocene, 1

A solution of 1,1′-bis(hydroxymethyl)ferrocene (0.5 g, 20.3 mmol) in dichloromethane (200 ml) and 2-mercaptopyridine (0.452 g, 40.6 mmol) in dichloromethane (200 ml) were added under N_2 to a stirred solution of trifluoroacetic acid (0.92 g, 80.7 mmol) in dichloromethane (100 ml). The reaction mixture was refluxed for 24 h and, after neutralizing

* Corresponding author.

PII S0022-328X(96)06954-9

Table 1
^{1}H NMR data for the ligands and their Zn^{2+} complexes

	$cp_{\alpha,\beta}$	CH_2	py-3 (py-3′)	py-4	py-5	py-6
1 [a]	4.22 t (J = 1.9 Hz), 4.12 t (J = 1.8 Hz)	4.21 s	7.26 d (J = 8.1 Hz)	7.63 tt	7.10 t	8.45 d (J = 4.1 Hz)
1:$Zn(CF_3SO_3)_2$ [a]	4.60 t (J = 1.8 Hz), 4.22 t (J = 1.8 Hz)	5.55 s	7.44 d (J = 7.7Hz)	7.27 tt	6.78 tt	8.18 d (J = 5.4 Hz)
2 [b]	4.15 t (J = 1.7 Hz), 4.09 t (J = 1.6 Hz)	3.87 s	7.15 m	7.60 m	7.15 m	8.41 d (J = 3.8 Hz)
2:$Zn(CF_3SO_3)_2$ [b]	4.39 br, 4.23 t (J = 1.9 Hz)	3.77 br	7.56 d (J = 7.4 Hz)	8.10 t	7.73 br	8.93 br
3 [b]	4.11 t, 4.05 t	3.46 s, 3.73 s	7.34 d (J = 7.4 Hz)	7.68 t	7.19 t	8.47 br
3:$Zn(CF_3SO_3)_2$ [b]	4.16 t, 4.11 t	3.46 s, 3.99 s	7.59 d (J = 7.8 Hz)	8.10 t	7.65 t	8.68 d (J = 5.2 Hz)
4 [c]	4.16 t (J = 1.7 Hz), 3.96 t (J = 1.7 Hz)	4.20 s	7.14 d (J = 7.7 Hz)	7.61 t (J = 7.7 Hz)	—	—
4:$Zn(CF_3SO_3)_2$ [d]	4.20 br, 3.90 br	4.55 br	8.00 d (J = 7.6 Hz)	8.59 t	—	—

[a] In DMSO-d_6; [b] in CD_3CN; [c] in $CDCl_3$; [d] in $CDCl_3$–CD_3CN.

with 10% KOH, the organic layer was washed with H_2O and dried ($MgSO_4$). Evaporation of the solvent gave a brown residue, which was recrystallised from acetonitrile to give **1** as light brown crystals (0.76 g, 87%), m.p. 79–82 °C; FAB: M^+ = 432. Found: C, 61.07; H, 4.55; N, 6.30. Calc. for $C_{22}H_{20}FeN_2S_2$: C, 61.11; H, 4.66; N, 6.48%. UV(CH_3CN): λ, 208, 252, 290, 440 nm (ε = 1891 mol^{-1} cm^{-1}).

The ^{1}H and ^{13}C NMR data are shown in Tables 1 and 2.

2.3. Synthesis of 1,1′-bis(2-picolylmercaptomethyl)ferrocene, 3

1,1′-Bis(2-picolylmercaptomethyl)ferrocene **3** was synthesised in an analogous reaction by condensation of 1,1′-bis(hydroxymethyl)ferrocene (0.275 g, 11.2 mmol) with 2-mercaptomethylpyridine (0.28 g, 22.3 mmol). The neutralised organic layer was washed, dried and evaporated to give a brown residue. Chromatography on silica (CH_2Cl_2–2% methanol) gave **3** as an orange-brown semi-solid (0.15 g, 30%). Exact mass determination by the chemical ionisation technique gave M = 460.0641; calculated mass for $C_{24}H_{24}N_2S_2Fe$: 460.0730. Elemental analysis was not satisfactory, possibly due to instability since the molecule decomposed slowly in solution. UV(CH_3CN): 460 nm (ε = 2741 mol^{-1} cm^{-1}).

The ^{1}H and ^{13}C NMR data are shown in Tables 1 and 2.

2.4. Synthesis of 1,1′-bis(2-thiomethylpyridino)ferrocene, 2

A degassed solution of aqueous sodium hydroxide (2.7 ml, 20%) was added to a solution of 1,1′-ferrocenedithiol (0.67 g, 2.7 mmol) in degassed absolute ethanol (20 ml). A solution of 2-bromomethylpyridine (0.92 g, 5.4 mmol) in ethanol (50 ml) was added dropwise to the stirred solution of sodium ferrocene dithiolate under N_2 and the mixture was stirred at room temperature for a further 24 h. Evaporation of the solvent gave a brown residue which was dissolved in water

Table 2
^{13}C NMR table for the ligands and their Zn^{2+} complexes

Ligands and their Zn^{2+} complexes	$cp_{a,b}$	γ	CH_2	C-2 (2′)	C-3 (3′)	C-4	C-5	C-6
1 [a]	69.6, 68.7	85.0	29.1	158.3	121.8	136.7	119.9	149.4
1:$Zn(CF_3SO_3)_2$ [a]	70.4, 69.2	83.2	53.5	178.4	134.7	134.7	113.7	141.4
2 [b]	75.4, 71.4	81.8	44.2	159.5	124.1	137.3	122.8	150.0
2:$Zn(CF_3SO_3)_2$ [b]	74.3, 73.0	75.8	42.4	155.4	128.1	142.5	126.2	149.4
3 [b]	70.4, 69.5	86.5	31.6 38.4	160.0	123.9	137.6	122.8	149.9
3:$Zn(CF_3SO_3)_2$ [b]	71.1, 70.5 70.3, 70.2	82.5 85.4	32.6 35.8	153.8	127.5	142.3	125.9	149.0
4 [c]	69.5, 66.7	90.6	38.8	157.9	120.3	137.1		
4:$Zn(CF_3SO_3)_2$ [d]	66.4, 68.4	86.6	34.9	149.2	126.1	148.6		

[a] In DMSO-d_6; [b] in CD_3CN; [c] in $CDCl_3$; [d] in $CDCl_3$–CD_3CN.

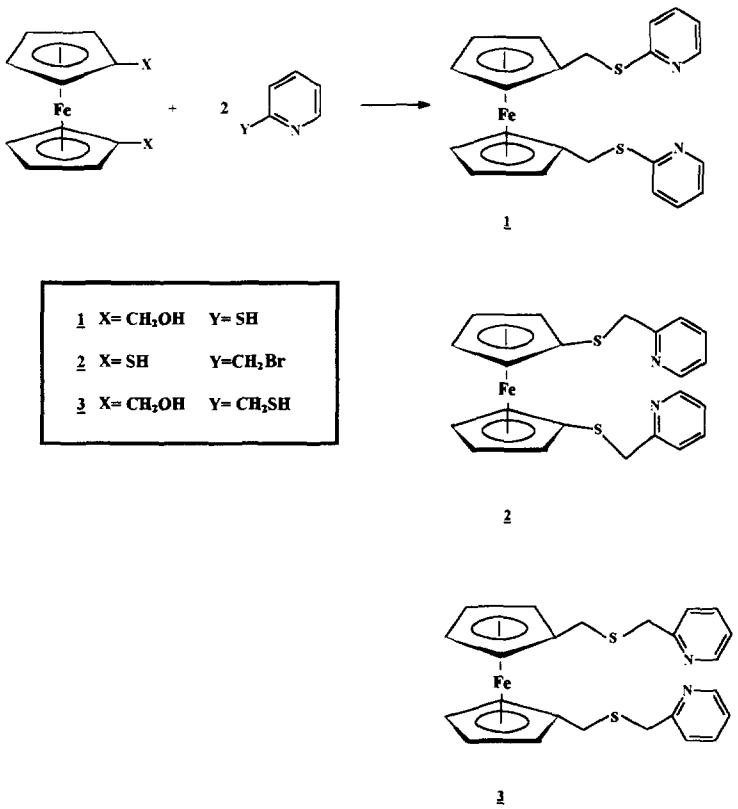

Scheme 1.

(200 ml) and extracted with diethyl ether (3 × 50 ml). The organic layer was dried ($MgSO_4$) and chromatographed on silica. Elution with CH_2Cl_2–1% MeOH gave a yellow oil from which the ligand (0.14 g, 12%) was isolated as yellow needles, m.p. 35–37 °C (CH_3CN). CI: (M + 1) = 433. Found: C, 61.04; H, 4.60; N, 6.29. Calc. for $C_{22}H_{20}FeN_2S_2$: C, 61.11; H, 4.66; N, 6.48%. UV(CH_3CN): λ, 198(sh), 212, 262, 440 nm (ε = 2671 mol^{-1} cm^{-1}).

^1H and ^{13}C NMR data are shown in Tables 1 and 2.

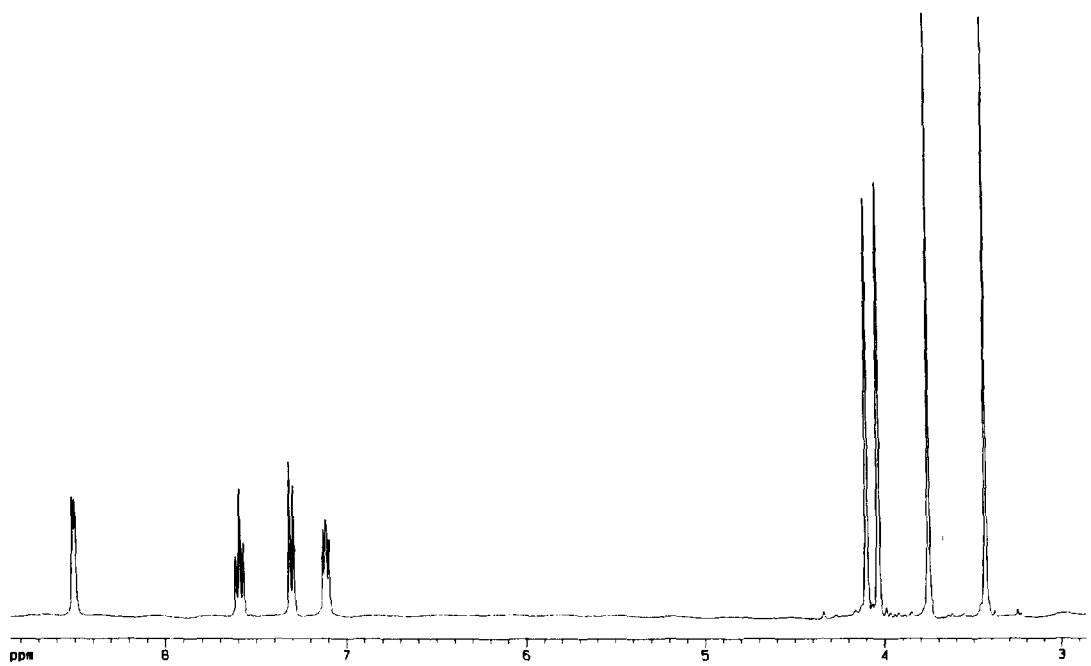

Fig. 1. ^1H NMR of ligand **3** in acetonitrile-d_3.

3. Results and discussion

3.1. Synthesis and characterisation of the ligands

Condensation of 1,1′-bis(hydroxymethyl)ferrocene and 2-mercaptopyridine in CH_2Cl_2 in the presence of trifluoroacetic acid gave 1,1′-bis(2-pyridylmercaptomethyl)ferrocene **1**. An analogous reaction with 2-mercaptomethylpyridine gave 1,1′-bis(2-picolylmercaptomethyl)ferrocene **3**. 1,1′-Bis(2-thiomethylpyridino) ferrocene **2** was prepared from the reaction of 1,1′-ferrocenedithiol with 2-bromomethylpyridine (see Scheme 1). The ligands were characterised by elemental analysis, mass spectrometry and NMR spectroscopy and as an example the ^1H NMR of **3** is shown in Fig. 1. For comparison of **1–3** with a macrocyclic ligand, 1,10-dithia[2](2,6)pyridino-ferrocenophane, **4** was synthesised, using the method described by Sato et al. [4].

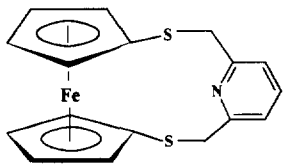

1

3.2. Coordination of the ligands with Zn^{2+} by NMR

Table 1 shows the ^1H data for the ligands and their 1:1 Zn^{2+} complexes in approximately 5×10^{-2} M solu-

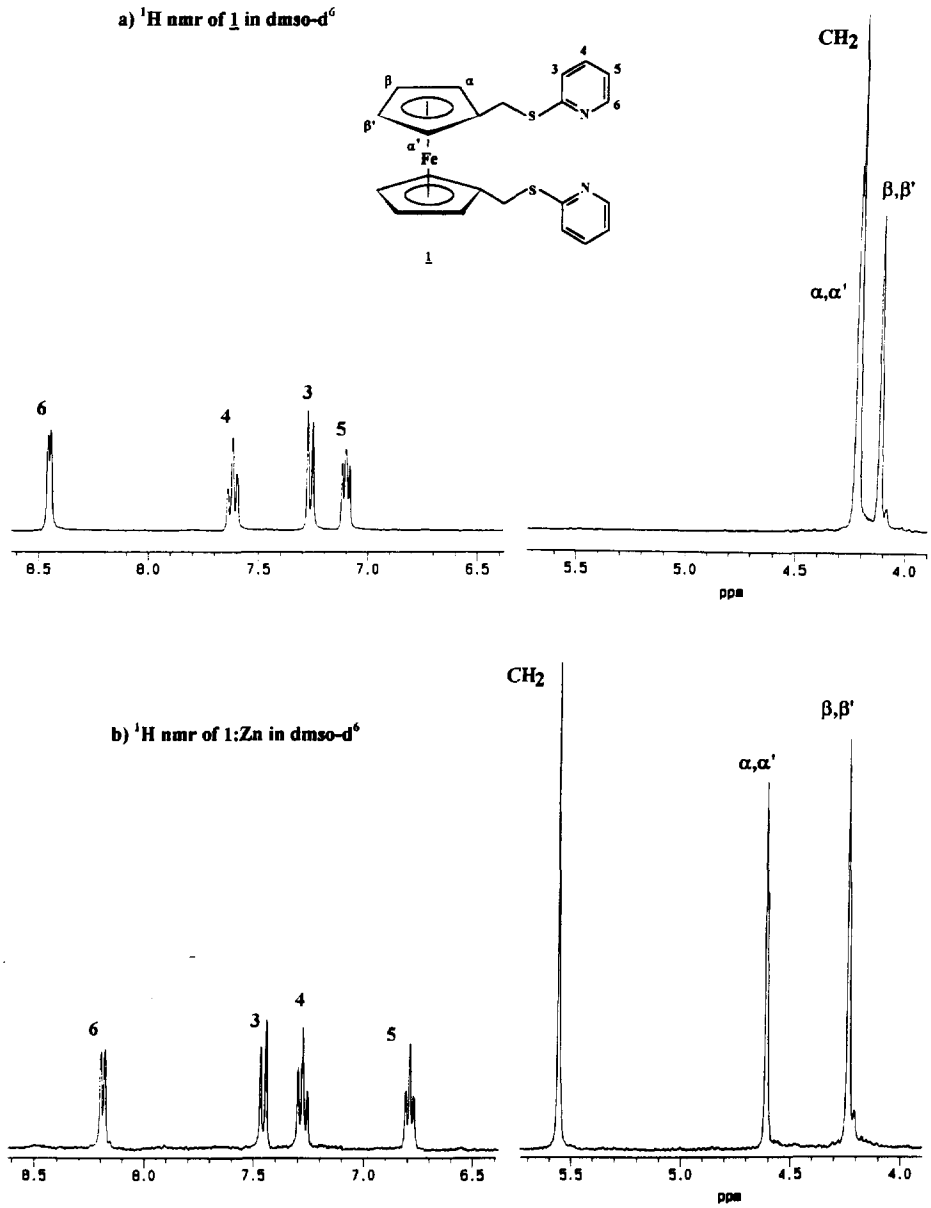

Fig. 2. ^1H NMR of ligand **1** and the $Zn(ClO_4)_2 \cdot 6H_2O$ complex: (a) **1** in DMSO-d_6; (b) **1**:Zn in DMSO-d_6.

tion. Zinc triflate, $Zn(CF_3SO_3)_2$, was dissolved in CD_3CN and was added to a solution of each ligand in CD_3CN. When zinc perchlorate, $Zn(ClO_4)_2 \cdot 6H_2O$, was used instead, chemical shifts were found to be independent of the nature of the counter ion. The zinc complex of **1** was isolated as a yellow microcrystalline material, which was dried and redissolved in DMSO-d_6 in order to record the NMR spectra. Assignments are based on the results of selective decoupling and CH correlation experiments.

In the ^1H spectra a substantial downfield shift ($\Delta\delta$ = 1.34 ppm) for the bridging methylene protons (δ 5.55) was observed (Fig. 2), compared to the free ligand (δ 4.21 ppm). Shifts to higher field for pyridine protons 4, 5 and 6 were also observed on complexation. Conversely, the pyridine proton 3 appears at lower field (δ 7.44) in the complex compared to 7.24 ppm in the free ligand. This proton, ortho to the pyridine–sulphur bond, is therefore strongly deshielded. Since the nitrogen/sulphur binding site in **1** is more restrained than in the other ligands, a dimeric structure $\{(\mathbf{1}{:}Zn)_2\}$ seems more likely for the zinc complex. This is consistent with the insolubility of the complex in almost every common solvent. Unfortunately, all attempts to obtain suitable crystals for structure determination by X-ray crystallography were unsuccessful.

In comparison, all the pyridine ring protons of the zinc complexes with **2**, **3** and **4** gave resonance signals at lower field than those of the free ligands, suggesting a very different coordination mode to that observed with **1**. Coordination of metals with the nitrogen atom of pyridine has been reported to displace the NMR signals for protons 4, 5 and 6 to lower field [10]. Complexation of **4** with palladium was reported to have a less drastic effect on the proton resonances of the pyridine ring and Pd^{2+} was found to be asymmetrically complexed by the macrocycle with a considerable degree of dative character in the Pd–Fe bond [2]. The complex of **4** with the smaller zinc ion is symmetric with only one broad peak appearing for the bridging methylene protons at lower field as found for the complex of Zn^{2+} with **1**. The bridging methylene protons of **2** and **3**, however, were only slightly shifted on complexation with Zn^{2+}.

The corresponding ^{13}C NMR data are reported in Table 2. For the complex of **1** a substantial downfield shift ($\Delta\delta$ = 20.1 ppm) was found for C-2, the *ipso*-pyridine carbon. In addition, carbon C-3 moved downfield by 12.9 ppm, whereas the remaining carbon signals of the pyridine ring moved slightly towards higher field. In agreement with the downfield shift for the methylene ^1H resonance, the carbon signal shifted dramatically, from 29.1 ppm in the free ligand to 53.5 ppm in the complex. We may assume, therefore, that there is a substantial conformational change within **1** on complexation.

The complexes from **2**, **3** and **4** showed remarkably different behaviour. The pyridine carbon (C-6) for **2** and **3** remained virtually unchanged on complexation and carbons C-3, C-4 and C-6 generally moved downfield by 4–6 ppm. Pyridine carbon (C-2), however, moved upfield by 6–9 ppm and the γ carbon of the cp ring also moved upfield (4–6 ppm) in each case. The methylene carbons moved upfield slightly on complexation and the cp (CH) carbons remained almost unchanged. The overall conclusion, therefore, is that complexation of **2** and **3** with Zn^{2+} is very similar to that found with **4**. Thus it is likely that the relative geometry of the coordinating atoms (three bonds between S and N in **2**, **3** and **4** but only two bonds in **1**) has a very profound effect on the coordination behaviour of the ligands.

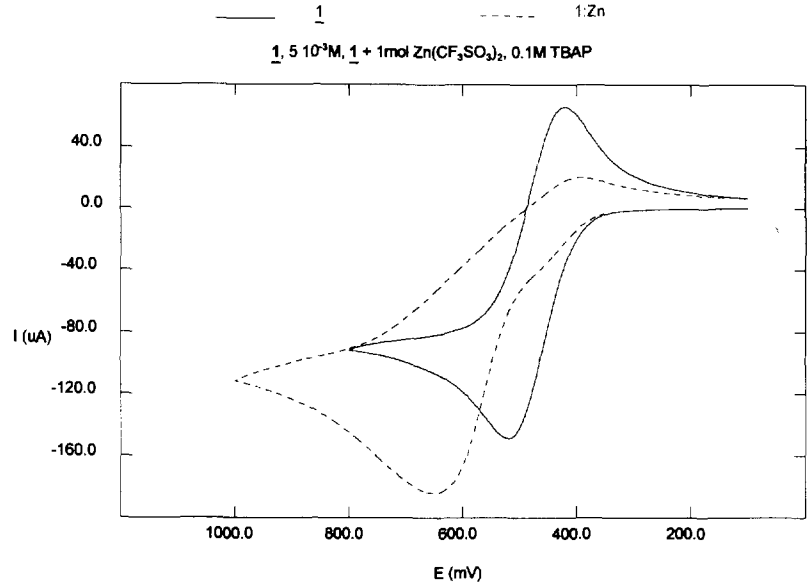

Fig. 3. Cyclic voltammogram of ligand **1** and the Zn^{2+} complex in acetonitrile (vs. Ag/AgCl).

3.3. Coordination studies by cyclic voltammetry

The electrochemical data for ligands **1–4** and their zinc complexes are summarised in Table 3. The reversible oxidation process due to the ferrocene/ferrocenium couple for the ligands **1**, **2**, **3** is shown to be anodically shifted by about 50 mV compared to unsubstituted ferrocene. The redox wave was shown to be reversible by the criteria of $(E_{pa} - E_{pc}) \sim 60$ mV, $i_{pa} = i_{pc}$ and a plot of i_{pc} vs. (scan rate)$^{1/2}$ being linear. The instability of **3** might explain a second oxidation peak appearing at higher anodic potential in the cyclic voltammogram of the ligand. Interaction between the sulphur and the ferrocene nucleus results in a more negative (cathodic shift) redox potential for **4** [11].

Subsequent addition of aliquots of zinc triflate introduced an anodic shift of the redox potential with no further change beyond 1:1 molar ratio for all the ligands. These data suggest the formation of 1:1 complexes with Zn^{2+}. Fig. 3 shows the irreversible wave of **1**:$Zn(CF_3SO_3)_2$ which points to an instability or possible lability of the $[\mathbf{1}{:}Zn(CF_3SO_3)_2]^+$ species. In contrast, a reversible oxidation process was observed for **2**:$Zn(CF_3SO_3)_2$ which is shown in Fig. 4. No electrochemical data on the zinc complex of **3** could be obtained due to deposition on the platinum electrode. For the Zn^{2+} complex of **4** a shift of $\Delta E_{1/2}$ of 0.21 V was observed compared to 0.09 V for **2**:Zn^{2+}. Ferrocene derivatives with 1,1′-substituted sulphur coordination atoms form strong complexes with Pd and Pt where dative bonds between Fe and the transition metal have been observed [12]. No interaction between the iron centre and complexed zinc was observed, since a contribution from a dative bond would cause larger changes in the electrode potentials.

Table 3
Redox potentials in acetonitrile vs. Ag/AgCl (conc.: 5×10^{-3} M, 0.1 M Bu_4NClO_4; working electrode: Pt)

	E_{pa} (V)	E_{pc} (V)	$E_{1/2}$ (V)	$\Delta E_{1/2}$ (mV) [c]
1	+0.52	+0.42	+0.47	
1:$Zn(CF_3SO_3)_2$	+0.65	—	+0.65	+180
1:$Cu(CF_3SO_3)_2$	+0.59	+0.45	+0.52	+50
1:CuBr	+0.49	+0.40	+0.44 [a]	−30
2	+0.50	+0.41	+0.46	
2:$Zn(CF_3SO_3)_2$	+0.62	+0.48	+0.55	+90
3	+0.49	+0.39	+0.44 [b]	
	+0.71	+0.62Sh	+0.66	
4	+0.29	+0.19	+0.24	
4:$Zn(CF_3SO_3)_2$	+0.51	+0.40	+0.45	+210

[a] Second less-intensive wave observed at $E_{1/2}$ value assigned to Cu^{2+}/Cu^+ couple.
[b] Ligand is unstable.
[c] $\Delta E_{1/2} = E_{1/2}$(complex) − $E_{1/2}$(ligand).

Since the zinc complex of ligand **1** gave rise to an irreversible oxidation wave we studied the change in the redox behaviour with different ions. Table 3 also shows the results for the Cu^{2+} and Cu^+ complexes. Copper(II) changed the ferrocene-centred oxidation to 0.5 V, giving rise to a quasi-reversible wave with $E_{pa} - E_{pc} =$ 140 mV. A small cathodic shift occurred after addition of aliquots of cuprous bromide with the shift again maximizing at a 1:1 molar equivalent.

In order to confirm the composition of the complexes the change in the absorbance of the d–d transition (ca. 420–460 nm, $\varepsilon \sim 250$ l mol^{-1} cm^{-1}) of each ligand was observed on titrating solutions of the ligands with zinc triflate. For each ligand a linear relationship between

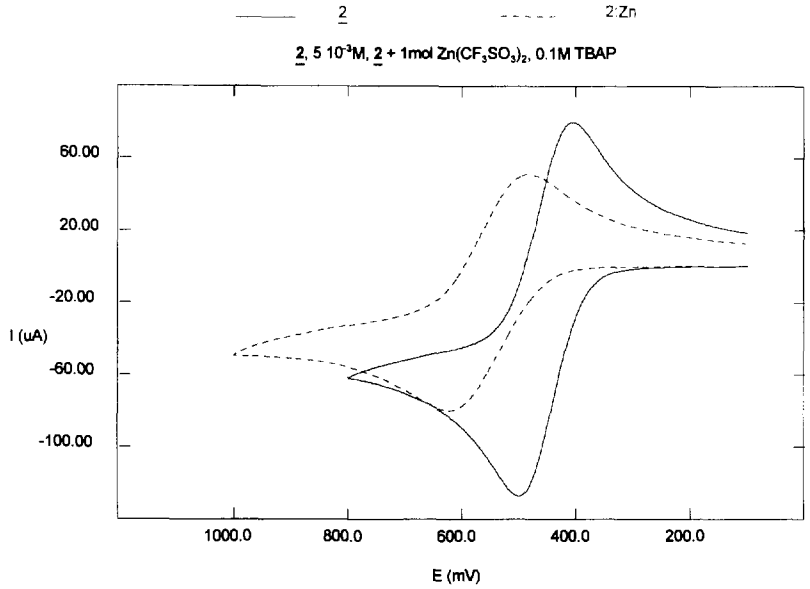

Fig. 4. Cyclic voltammogram of ligand **2** and the Zn^{2+} complex in acetonitrile (vs. Ag/AgCl).

the absorbance change and molar concentration was found, which again maximised at a 1:1 molar stoichiometry in ligand to zinc concentration. The molar extinction coefficient ε increased for **1** and **4**, but decreased on addition of Zn^{2+} to **2** and **3**.

4. Conclusions

Three N,S-containing ferrocene ligands have been characterised and their complexation behaviour towards Zn^{2+} investigated. Incorporation of a methylene bridge between sulphur and pyridine unit changes the complexation pattern.

Shifts in the NMR spectra suggest coordination via the pyridine nitrogen for all the ligands and electrochemical and UV absorbance data imply a 1:1 complexation stoichiometry.

Acknowledgements

We wish to thank Jotun Protective Coatings for a studentship (to N.S.).

References

[1] (a) M.D. Rausch and D.J. Ciapenelli, *J. Organomet. Chem., 10* (1967) 127. (b) J.S. Kim, A.J. Bessire, R.A. Bartsch, R.A. Holwerda and B.P. Czech, *J. Organomet. Chem., 484* (1994) 47.
[2] M. Sato, H. Asano and S. Akabori, *J. Organomet. Chem., 452* (1993) 105.
[3] N. Sachsinger and C.D. Hall, *J. Organomet. Chem.*, in press.
[4] M. Sato, S. Tanaka, S. Ebine, K. Morinaga and S. Akabori, *J. Organomet. Chem., 289* (1985) 91.
[5] U.T. Mueller-Westerhoff, Z. Yang and G. Ingram, *J. Organomet. Chem., 463* (1993) 163. K.L. Rinehart, Jr., A.K. Frerichs, P.A. Kittle, L.F. Westman, D.H. Gustafson, R.L. Pruett and J.E. McMahon, *J. Am. Chem. Soc., 82* (1960) 4111.
[6] J.J. Bishop, A. Davison, M.L. Katcher, D.W. Lichtenberg, R.E. Merill and R.F. Bryan, *J. Organomet. Chem., 27* (1971) 241.
[7] B.R. Brown and J. Humphreys, *J. Chem. Soc.*, (1959) 2040.
[8] E. Maruszewska-Wieczorkowska and J. Michalski, *Rocniki Chem., 31* (1957) 543.
[9] H.S. Mosher and J.E. Tessieri, *J. Am. Chem. Soc., 73* (1951) 4925.
[10] K. Tani, T. Mihana, T. Yamagata and T. Saito, *Chem. Lett.*, (1991) 2047.
[11] M. Sato, K. Suzuki, H. Asano, M. Sekino, Y. Kawata, Y. Habata and S. Akabori, *J. Organomet. Chem., 470* (1994) 263.
[12] B. McCulloch, D.L. Ward, J.D. Woolins and C.H. Brubaker, Jr., *Organometallics, 4* (1985) 1425.